CHEMMEDCHEM

DOI: 10.1002/cmdc.200800039

Cellular Uptake, Cytotoxicity, and Metabolic Profiling of Human Cancer Cells Treated with Ruthenium(II) Polypyridyl Complexes $[Ru(bpy)_2(N–N)]Cl_2$ with N–N = bpy, phen, dpq, dppz, and dppn**

Ulrich Schatzschneider,*[a] Johanna Niesel,[a] Ingo Ott,*[b] Ronald Gust,[b] Hamed Alborzinia,[c] and Stefan Wölfl*[c]

A series of five ruthenium(II) polypyridyl complexes $[Ru(bpy)_2(N–N)]Cl_2$ was tested against human HT-29 and MCF-7 cancer cell lines. Cellular uptake efficiency and cytotoxicity were found to increase with the size of the aromatic surface area of the N–N ligand. The most active compound carrying the dppn ligand exhibits a low micromolar IC_{50} value against both cell lines comparable to that of cisplatin under similar conditions. Continuous measurement of oxygen consumption, extracellular acidification rate, and impedance of the cell layer with a chip-based sensor system upon exposure to the complexes showed only small changes for the first two parameters throughout the series. A significant and irreversible decrease in impedance was, however, found for the dppn compound. This suggests that its biological activity is related to modifications in cell morphology or cell–cell and cell–matrix contacts.

Introduction

In the search for metal-based therapeutic agents against cancer, ruthenium plays a very important role[1–3] and is probably only surpassed by platinum in the number of studies reported so far.[4–6] Most advanced toward clinical applications in humans are some ruthenium(III) chlorido complexes such as indazolium [*trans*-tetrachloridobis(1*H*-indazole)ruthenate(III)], KP1019, and imidazolium [*trans*-tetrachlorido(dimethyl sulfoxide)(imidazole)ruthenate(III)], NAMI-A. The former compound shows promising effects in a variety of tumor models, including colorectal carcinoma in rat, and has already successfully completed phase I clinical trials,[7] whereas the latter, although inactive against primary tumor cells, efficiently decreases the formation and growth of metastases.[8]

Ruthenium(II) complexes have also found widespread interest in medicinal inorganic chemistry. Compounds carrying labile ligands such as α-$[Ru(azpy)_2Cl_2]$ (azpy = 2-phenylazopyridine) undergo hydrolysis and subsequently bind to the constituents of bio(macro)molecules.[9] Some of them show a cytotoxic potential similar to or even better than that of cisplatin.[10–12] Organometallic arene ruthenium compounds of the general formula $[Ru(\eta^6\text{-arene})(L)(L')(L'')]X_n$, in which at least some of the ligands L are labile, have also received a lot of attention recently, with structure–activity studies against a variety of cancer cells lines reported.[13–17] In addition to such complexes capable of covalently binding to bio(macro)molecules, coordinatively saturated and substitutionally inert ruthenium(II) compounds have also received enormous attention. Because they can only form noncovalent adducts, a large number of studies have been devoted to the investigation of their groove-binding and intercalative interactions with DNA.[18–20] Surprisingly, however, little is known about their in vitro behavior. Only a few studies have focused on their intracellular accumulation and antiproliferative properties.[21–25] We therefore decided to carry out a systematic evaluation of a series of ruthenium complexes $[Ru(bpy)_2(N–N)]Cl_2$ **1**–**5** (Figure 1) with aromatic bidentate ligands (N–N = bpy, phen, dpq, dppz, and dppn) to study the influence of ligand surface area on cellular uptake efficiency and cytotoxicity. Additionally, a chip-based sensor system was used to continuously monitor three key metabolic parameters: oxygen consumption, extracellular acidification rate, and impedance as an indicator of changes in cell morphology and adhesion properties, to get more detailed insight into the biological mode of action of these compounds.

[a] *Dr. U. Schatzschneider, J. Niesel*
Lehrstuhl für Anorganische Chemie I – Bioanorganische Chemie
Ruhr-Universität Bochum NC 3/74
Universitätsstr. 150, 44801 Bochum (Germany)
Fax: (+49) 234-32-14378
E-mail: ulrich.schatzschneider@rub.de

[b] *Dr. I. Ott, Prof. Dr. R. Gust*
Institut für Pharmazie, Freie Universität Berlin
Königin-Luise-Str. 2+4, 14195 Berlin (Germany)
Fax: (+49) 30-838-56906
E-mail: ottingo@zedat.fu-berlin.de

[c] *H. Alborzinia, Prof. Dr. S. Wölfl*
Institut für Pharmazie und Molekulare Biotechnologie – Abteilung Biologie
Ruprecht-Karls-Universität Heidelberg
Im Neuenheimer Feld 346, 69120 Heidelberg (Germany)
Fax: (+49) 6221-54-4884
E-mail: stefan.wolfl@uni-hd.de

[**] *bpy = 2,2′-bipyridine, phen = 1,10-phenanthroline, dpq = dipyrido[3,2-f:2′,3′-h]quinoxaline, dppz = dipyrido[3,2-a:2′,3′-c]phenazine, dppn = 4,5,9,16-tetraazadibenzo[a,c]naphthacene*

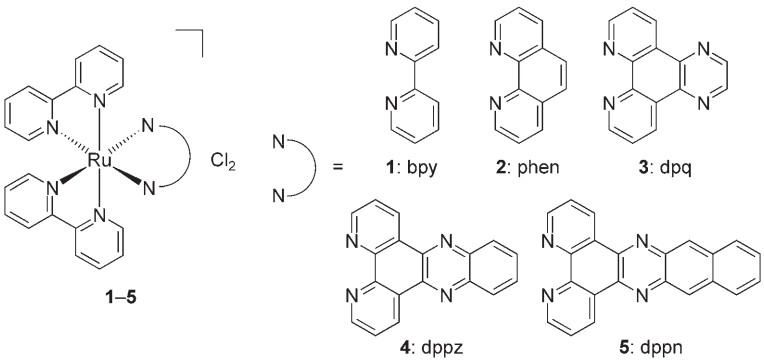

Figure 1. Ruthenium complexes **1**–**5** investigated in this study.

Results

Synthesis

All five ruthenium complexes **1**–**5** (Figure 1) studied in this work were prepared in a similar way by reaction of $[Ru(bpy)_2Cl_2]\cdot 2H_2O$ with bidentate N–N ligands bpy, phen, dpq, dppz, and dppn in ethanol/water (1:1 *v/v*) at reflux for five hours. They were then precipitated from an aqueous solution with saturated ammonium hexafluorophosphate. This material was redissolved in acetone and produced the chloride salts as crystalline solids upon addition of tetra-*n*-butylammonium chloride. All analytical data are in full accordance with the expected composition and in line with those reported in the literature.[26–32]

Cellular uptake

For coordinatively saturated and substitutionally inert ruthenium(II) polypyridyl complexes, noncovalent association with DNA is generally assumed to be the primary mode of interaction with biological systems. Especially compounds carrying ligands with an extended aromatic surface area such as dppz and dppn, as in **4** and **5**, are thought to predominantly bind through intercalation into the DNA base stack.[18–20] To exert this action in vitro and in vivo, efficient intracellular accumulation is required. Cultures of human colon and breast cancer cell lines HT-29 and MCF-7, respectively, were thus treated for several hours with solutions of complexes **1**–**5**. NAMI-A was also evaluated under identical conditions as an established ruthenium-containing reference drug. After replacement with pure buffer and subsequent washing steps, the cellular ruthenium content of the samples was determined by graphite furnace atomic absorption spectroscopy (GF-AAS), and the protein content by the Bradford method. Results are reported herein as ng ruthenium per mg cellular protein. Importantly, this method gives reproducible results on metal association with cells when applied to other metals as well,[33] but it does not allow one to distinguish between the metal complexes that are internalized in vesicles, released to the cytosol, or that remain tightly associated with the cellular membrane.

Low uptake levels were noted for **1**–**4** and NAMI-A (Table 1). An incubation concentration of 500 μM had to be used for these complexes to reach detectable cellular Ru levels. The result that clearly stands out, however, is the elevated uptake of the dppn compound **5**, which shows Ru levels >100 ng Ru per mg cell protein in both cell lines at exposure to 100 μM complex. In this context it should be noted that cells treated with **5** could not be isolated following the established procedure based on enzymatic digestion of the extracellular matrix with trypsin. Instead, the cells remained attached to the bottom of the culture flasks and had to be scraped off mechanically. This observation is a first indicator that **5** probably modifies the cell–cell or cell–matrix adhesion properties, which is also reflected in the impedance measurements (see below). Evaluation of the data obtained for **1**–**5** shows a clear correlation between the size of the aromatic surface area of the N–N ligand and the amount of ruthenium associated with the cells. Thus, enlargement of the aromatic ring system results in an increase in the cellular Ru levels. A recent combined flow cytometry and confocal microscopy study on **4** and analogues with substituted bipyridines as co-ligands using HeLa cells also showed efficient cellular uptake. The latter method provided clear evidence that at least part of the compound is indeed transported to the interior of the cells instead of remaining associated only with the cell membrane.[23] The immediate onset of effects on key cellular metabolic parameters (see below), however, suggests that an intracellular or even intranuclear accumulation of compound **5** is not required to exert its action.

Table 1. Cellular uptake and cytotoxicity of ruthenium complexes **1**–**5**, NAMI-A, and cisplatin against HT-29 and MCF-7 human cancer cell lines.

	HT-29		MCF-7	
Compd	Ru [ng mg^{-1}][a]	IC_{50} [μmol L^{-1}]	Ru [ng mg^{-1}][a]	IC_{50} [μmol L^{-1}]
1	5.2 ± 6.0[b]	32.3 ± 8.4	8.5 ± 3.3[b]	778.3 ± 107.2
2	15.1 ± 6.7[b]	119.4 ± 10.8	15.0 ± 9.3[b]	122.5 ± 9.5
3	20.7 ± 4.2[b]	62.1 ± 3.9	9.9 ± 4.8[b]	51.8 ± 2.2
4	38.8 ± 3.1[b]	26.9 ± 0.4	47.8 ± 8.8[b]	90.2 ± 19.6
5	162.7 ± 3.0[c]	6.4 ± 1.9	128.2 ± 2.7[c]	3.3 ± 1.2
NAMI-A	12.8 ± 7.7[b]	513 ± 24	28.6 ± 6.5[b]	591 ± 63
cisplatin	n.d.[d]	7.0 ± 2.0[17]	n.d.[d]	2.0 ± 0.3[17]

[a] Ru concentration in ng per mg cell protein. [b] Ru exposure concentration: 500 μmol L^{-1}. [c] Ru exposure concentration: 100 μmol L^{-1}. [d] Not determined.

Cytotoxicity

Having established an efficient cellular uptake in HT-29 and MCF-7 cells at least for the largest member of the series of compounds **5**, we then proceeded to study the effect on cell viability using crystal violet staining of the cell biomass after incubation for up to 96 h in the presence of complexes **1**–**5**. IC_{50} values determined from these experiments are listed in Table 1.

In good agreement with the cellular uptake data, low antiproliferative effects (IC_{50} values $>25\,\mu M$) were noted for **1**–**4**. In contrast, the dppn compound **5** was significantly more active in both cell lines studied (IC_{50} values $<10\,\mu M$) and showed an IC_{50} value similar to that of cisplatin under identical conditions.[17] With the exception of **1** in HT-29, the cell growth inhibitory potency increases with increasing aromatic surface area of the bidentate N–N ligand. As expected, NAMI-A was completely inactive (IC_{50} values $>500\,\mu M$) in this in vitro assay. This is in line with a series of previous studies which showed that it acts only on metastases but not primary tumor cells.[8] It is thus interesting to find a level of cytotoxicity for the most active of these coordinatively saturated and substitutionally inert ruthenium(II) polypyridyl complexes such as **5** that is similar to that of cisplatin, a classic anticancer agent which covalently binds DNA after hydrolysis of its labile ligands. It should be noted that high cytotoxicities against these two cell lines in the low micromolar range were also recently reported for dppn arene ruthenium and Cp* iridium complexes.[17]

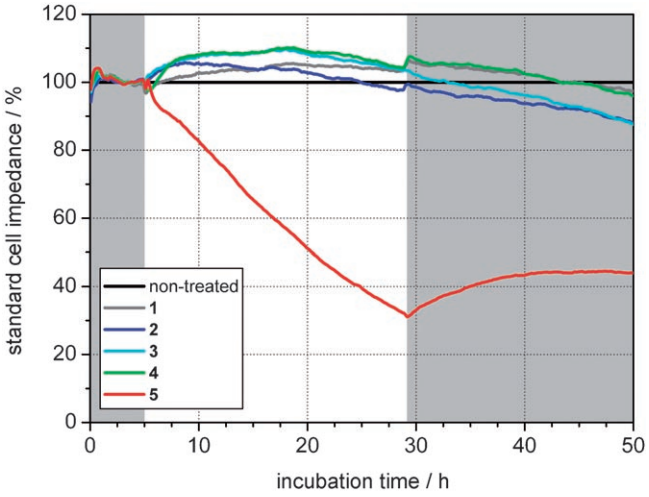

Figure 2. Standard cell impedance expressed as percentage relative to a non-treated control chip for HT-29 colon cancer cells exposed to medium (gray shaded area) or medium containing compounds **1**–**5** (white area).

Cellular metabolism

To gain insight into the mode of action of compounds **1**–**5**, we then studied the immediate effect on cellular metabolism and morphology of HT-29 colon cancer cells in response to exposure to each of the five compounds at $100\,\mu M$ using a chip-based sensor system (Bionas 2500). This allows one to monitor important metabolic parameters of living cells such as oxygen consumption, extracellular acidification rate, and changes in cellular morphology and adhesion properties over an extended time span. The chip contains ion-sensitive field effect transistors (ISFETs) to measure extracellular pH, Clark-type oxygen electrodes to follow cellular oxygen uptake, and interdigitated electrode structures (IDES) for impedance measurements.[34–36]

The acidification rate of the medium is closely linked to cellular energy metabolism, respiration, and glycolysis through the dominant contribution of lactic acid production into the extracellular environment. The rate of oxygen consumption is an indicator of mitochondrial activity, dependent on the citrate cycle, and ATP production in the respiratory chain. Finally, the impedance of the cell layer growing on the chip surface is influenced by the insulating properties of the cell membrane. This allows one to detect changes in cell morphology and adhesion properties like cell–cell and cell–matrix contacts.

During analysis the medium was exchanged in cycles of 4 min while changes in the parameters were recorded. Treatment with compounds **1**–**5** started after an equilibration period of five hours and was continued for 24 h. Afterwards, the cells were allowed to recover in pure growth medium for another 21 h.

As shown in Figure 2, the HT-29 cells clearly respond to application of all five compounds by changes in cell impedance. Also, the onset of the recovery period results in a discontinuity in the curves. Whereas the effects are very small for compounds **1**–**4**, a dramatic decrease in cell impedance by almost 70% is observed for dppn complex **5**. This is a clear indication of significant changes in cell morphology and adhesion properties. The modifications of the cells are irreversible in this case, as the impedance hardly recovers when the cells are resupplied with pure growth medium. The data, however, do not allow one to distinguish between either a direct membrane effect or the interaction of **5** with membrane proteins.

The extracellular acidification rate, as shown in Figure 3, slightly decreases during exposure to compounds **1**–**5** in a comparable manner. While in the case of **1**–**4**, cells somewhat recover when growth medium without the compounds is resupplied after 24 h, treatment with dppn complex **5** has an irreversible effect on this parameter of cellular metabolism as well, as the acidification rate continues to decrease during the recovery period.

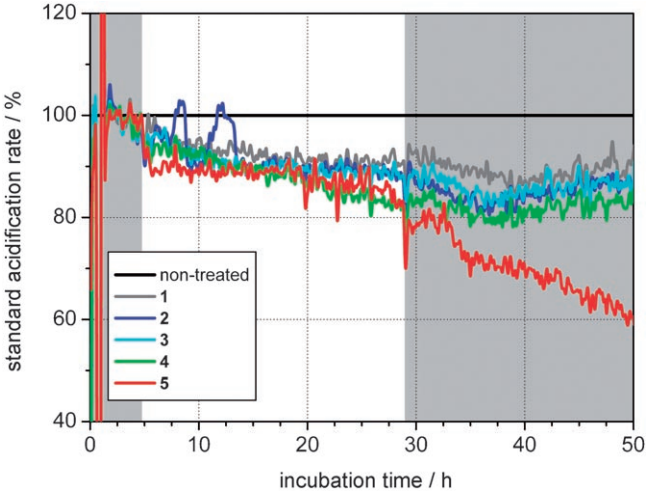

Figure 3. Standard extracellular acidification rate expressed as percentage relative to a non-treated control chip for HT-29 colon cancer cells exposed to medium (gray shaded area) or medium containing compounds **1**–**5** (white area).

The respiration rate, which measures oxygen consumption by the cells, shows a less clear picture (Figure 4). Whereas **2** and **3** only marginally differ from control, **1** and **4** show a slight decrease over time. Compound **5** displays a very unstable behavior at the beginning of the treatment followed by a continuous increase through most of the incubation. Although the differences in the response allow no simple interpretation, the changes in oxygen consumption confirm the special behavior of **5** also observed in the impedance and acidification rate measurements.

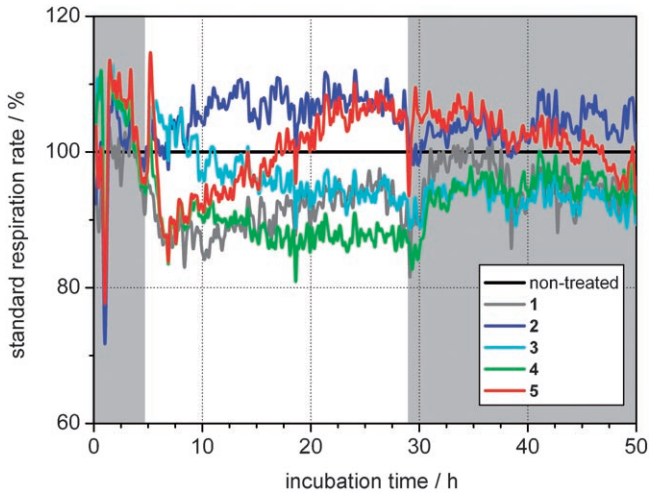

Figure 4. Standard respiration rate expressed as percentage relative to a non-treated control chip for HT-29 colon cancer cells exposed to medium (gray shaded area) or medium containing compounds **1**–**5** (white area).

Discussion

The cellular uptake efficiency of ruthenium complexes $[Ru(bpy)_2(N{-}N)]Cl_2$ **1**–**5** by HT-29 and MCF-7 human cancer cells in general shows a positive correlation with the increasing aromatic surface area of the bidentate N–N ligand. This is in line with the higher affinity of the more hydrophobic systems to the cell membrane and in good agreement with previous results on structurally related complexes.[17] Compound **5**, with the dppn ligand, is particularly efficient in associating with both types of cancer cells. Based on distinct cellular parameters such as cell volume and cell protein content of the MCF-7 and HT-29 cells,[33,37] the molar cellular ruthenium concentration can be estimated from the measured ng mg^{-1} values; 1 ng ruthenium per 1 mg cell protein corresponds to a complex concentration of 1.1 μM in MCF-7 and 2.0 μM in HT-29 cells. Accordingly, **5** reaches a concentration of 141 μM in MCF-7 and 325 μM in HT-29 cells, which is well above the exposure concentration (100 μM) in both cases. In contrast, the cellular levels obtained with **1**–**4** are significantly lower than the incubation concentration (500 μM), which results in the lower antiproliferative potencies of these complexes. Thus, more efficient cellular accumulation leads to higher cytotoxicity of the compounds against both cell lines. Again, dppn complex **5** clearly stands out, with IC_{50} values against HT-29 and MCF-7 cell lines in the low micromolar range and comparable to those obtained for cisplatin under identical conditions.

These results raise the question of the mode of action of compound **5**. Because it lacks labile ligands as found in many other classes of metallopharmaceuticals, formation of covalent adducts with bio(macro)molecules seems unlikely. Therefore, continuous profiling with a chip-based sensor system was used to monitor changes in key metabolic parameters such as oxygen consumption, extracellular acidification rate, and impedance as a measure of changes in cellular morphology and adhesion properties. The first two parameters underwent only small changes upon treatment of the cells with **5**, thus ruling out a major influence on the cellular energy metabolism and mitochondrial activity. On the other hand, the impedance decreased by almost 70% in an irreversible manner. The strong effect of **5** and the extremely low activity of **1**–**4** in the impedance measurements are in excellent agreement with the cytotoxicity and cellular uptake results of the complexes, indicating that a direct interaction of compound **5** with the constituents of the cell membrane or embedded membrane proteins could significantly contribute to the mode of action of **5**. This observation might also be relevant for other related cytotoxic ruthenium(II) polypyridyl complexes.

Conclusions

We have identified a coordinatively saturated and substitutionally inert ruthenium(II) polypyridyl complex with an extended aromatic ligand that exhibits cytotoxic activity against two cancer cell lines at low micromolar IC_{50} values. Our data point to a modification of cell membrane function and cell adhesion properties as the main mode of action. This contrasts with the conventional focus on the DNA-intercalating properties of such complexes. Further experiments are required to elucidate the precise mode of biological action of this complex and related compounds currently under study.

Experimental Section

General: Solvents were dried over molecular sieves and degassed prior to use when necessary. All chemicals were obtained from commercial sources and used without further purification. NMR spectra were recorded on Bruker DPX 200 and DRX 400 spectrometers (^{1}H at 200.13 and 400.13 MHz, respectively). Chemical shifts (δ in ppm) indicate a downfield shift relative to tetramethylsilane (TMS) and were referenced against the signal of the solvent.[38] Coupling constants J are given in Hz. Individual peaks are marked as: singlet (s), doublet (d), triplet (t) quartet (q), or multiplet (m). ESI mass spectra were measured on a Bruker Esquire 6000 instrument. The solvent flow rate was 8 μL min^{-1} with a nebulizer pressure of 20 psi and a dry gas flow rate of 7 L min^{-1} at a dry gas temperature of 350 °C. MS peak positions are reported for the most intense line of the isotope distribution observed.

Synthesis: The synthesis of $[Ru(bpy)_2(dpq)]Cl_2$ **3** is described as an example: bis(2,2′-bipyridine)dichloridoruthenium(II) dihydrate (289 mg, 0.56 mmol) and dipyrido[3,2-*f*:2′,3′-*h*]quinoxaline (359 mg, 1.55 mmol) were suspended in a degassed mixture of EtOH/H_2O

(1:1 *v/v*) and then heated at reflux under argon in the absence of light for 5 h. The clear orange solution thus obtained was cooled to room temperature and NH_4PF_6 (2.0 g) was added to precipitate the complex, which was collected on a sintered glass filter, washed with H_2O and Et_2O, and finally dried in air. The PF_6 salt was dissolved in a minimum amount of acetone, filtered, and then precipitated by the addition of a saturated solution of tetra-*n*-butylammonium chloride in acetone. The product was collected on a sintered glass filter, washed with a small quantity of ice-cold acetone, and dried in air overnight. NAMI-A was prepared by the procedure reported by Mestroni et al., and showed analytical data in full accordance with the literature.[39]

$[Ru(bpy)_3]Cl_2$ **1**: orange solid (199 mg, yield 39%); MS (ESI+, H_2O): $m/z = 284.97$ $[Ru(bpy)_3]^{2+}$; ^{1}H NMR (D_2O): $\delta = 8.56$ (d, 2H, $^3J = 8.1$ Hz, bpy H3), 8.06 (dt, 2H, $^3J = 7.9$ Hz, $^4J = 1.6$ Hz, bpy H4), 7.85 (d, 2H, $^3J = 5.7$ Hz, bpy H6), 7.39 ppm (ddd, 2H, $^3J = 7.7$ Hz, $^3J = 5.8$ Hz, $^4J = 1.3$ Hz, bpy H5); $[Ru(bpy)_2(phen)]Cl_2$ **2**:[26] orange solid (224 mg, yield quantitative), MS (ESI+, H_2O): $m/z = 297.00$ $[Ru(bpy)_2(phen)]^{2+}$; ^{1}H NMR ([D_6]DMSO): $\delta = 8.91$ (d, 2H, $^3J = 8.4$ Hz, bpy H3′), 8.86 (d, 2H, $^3J = 8.4$ Hz, bpy H3), 8.81 (d, 2H, $^3J = 8.0$ Hz, phen H4+H7), 8.39 (s, 2H, phen H5+H6), 8.22 (t, 2H, bpy, $^3J = 7.8$ Hz, bpy H4′), 8.13 (d, 2H, $^3J = 5.2$ Hz, phen H2+H9), 8.10 (d, 2H, $^3J = 8.0$ Hz, bpy H4), 7.89 (dd, 2H, $^3J = 8.0$ Hz, $^3J = 5.2$ Hz, phen H3+H8), 7.85 (d, 2H, $^3J = 5.6$ Hz, bpy H6′), 7.55–7.65 (m 4H, bpy H5′, H6), 7.35 ppm (dd, 2H, $^3J = 7.2$ Hz, $^3J = 6.0$ Hz, bpy H5); $[Ru(bpy)_2(dpq)]Cl_2$ **3**:[27–29,31] red solid (294 mg, yield 73%), MS (ESI+, H_2O): $m/z = 323.01$ $[Ru(bpy)_2(dpq)]^{2+}$; ^{1}H NMR (D_2O): $\delta = 9.47$ (dd, 2H, $^3J = 8.4$ Hz, $^4J = 1.2$ Hz, dpq H5+H12), 9.21 (s, 2H, dpq H2+H3), 8.67 (d, 2H, $^3J = 8.0$ Hz, bpy H3′), 8.64 (d, 2H, $^3J = 8.0$ Hz, bpy H3), 8.37 (dd, 2H, $^3J = 5.4$ Hz, $^4J = 1.4$ Hz, dpq H7+H10), 8.19 (dt, 2H, $^3J = 8.0$ Hz, $^4J = 1.2$ Hz, bpy H4′), 8.09 (dt, 2H, $^3J = 8.0$ Hz, $^4J = 1.6$ Hz, bpy H4), 8.02 (dd, 2H, $^3J = 5.6$ Hz, $^4J = 0.8$ Hz, bpy H6′), 7.92 (dd, 2H, $^3J = 8.4$ Hz, $^3J = 5.2$ Hz, dpq H6+H11), 7.81 (dd, 2H, $^3J = 5.6$ Hz, $^4J = 0.8$ Hz, bpy H6), 7.54 (ddd, 2H, $^3J = 7.6$ Hz, $^3J = 5.8$ Hz, $^4J = 1.4$ Hz, bpy H5′), 7.32 ppm (ddd, 2H, $^3J = 7.7$ Hz, $^3J = 5.9$ Hz, $^4J = 0.7$ Hz, bpy H5); $[Ru(bpy)_2(dppz)]Cl_2$ **4**:[30,32] dark red solid (88 mg, yield quantitative); MS (ESI+, H_2O): $m/z = 348.01$ $[Ru(bpy)_2(dppz)]^{2+}$; ^{1}H NMR (D_2O): $\delta = 8.98$ (d, 2H, $^3J = 8.0$ Hz, bpy H3′), 8.62 (dd, 4H, $^3J = 8.2$ Hz, $^3J = 4.2$ Hz, dppz H1+H8, bpy H3), 8.23 (dd, 2H, $^3J = 5.2$ Hz, $^4J = 0.8$ Hz, bpy H6′), 8.13 (dt, 2H, $^3J = 8.0$ Hz, $^4J = 1.2$ Hz, bpy H4′), 8.06 (dt, 2H, $^3J = 8.0$ Hz, $^4J = 0.8$ Hz, bpy H4), 7.91–8.00 (m, 4H, bpy H6, dppz H11+H12), 7.88 (d, 2H, $^3J = 5.2$ Hz, dppz H3+H6), 7.82 (dd, 2H, $^3J = 6.6$ Hz, $^3J = 3.4$ Hz, dppz H10+H13), 7.64 (dd, 2H, $^3J = 8.2$ Hz, $^3J = 5.4$ Hz, dppz H2+H7), 7.47 (dt, 2H, $^3J = 6.7$ Hz, $^4J = 0.7$ Hz, bpy H5′), 7.37 ppm (t, 2H, $^3J = 6.6$ Hz, bpy H5); $[Ru(bpy)_2(dppn)]Cl_2$ **5**: brown solid (204 mg, yield 76%), MS (ESI+, H_2O): $m/z = 373.01$ $[Ru(bpy)_2(dppn)]^{2+}$; ^{1}H NMR ([D_6]DMSO): $\delta = 9.63$ (dd, 2H, $^3J = 8.2$ Hz, $^4J = 1.4$ Hz, dppn H1+H8), 9.26 (s, 2H, dppn H10+H15), 8.90 (m, 4H, bpy H3, H3′), 8.46 (dd, 2H, $^3J = 6.6$ Hz, $^3J = 3.4$ Hz, dppn H11+H14), 8.21–8.25 (m, 4H, bpy H4′, dppn H3+6), 8.15 (dt, 2H, $^3J = 7.9$ Hz, $^4J = 1.3$ Hz, bpy H4), 8.03 (dd, 2H, $^3J = 8.2$ Hz, $^3J = 5.4$ Hz, dppn H2+H7), 7.78–7.84 (m, 6H, dppn H12+H13, bpy H6+H6′), 7.61 (ddd, 2H, $^3J = 7.6$ Hz, $^3J = 5.8$ Hz, $^4J = 1.4$ Hz, bpy H5′), 7.41 ppm (ddd, 2H, $^3J = 7.4$ Hz, $^3J = 5.8$ Hz, $^4J = 1.4$ Hz, bpy H5).

Cell culture: HT-29 human colon carcinoma and MCF-7 human breast cancer cells were maintained in cell culture medium (minimum essential Eagle's medium supplemented with 2.2 g sodium hydrogen carbonate, 110 mg L^{-1} sodium pyruvate, and 50 mg L^{-1} gentamicin sulfate adjusted to pH 7.4 and treated with 10% (*v/v*) fetal calf serum (FCS) prior to use) at 37 °C under 5% CO_2, and passaged twice a week according to standard procedures.

Cellular uptake: For cellular uptake studies, cells were grown to at least 70% confluency in 175-cm^3 cell culture flasks. Stock solutions of the complexes in dimethyl sulfoxide (DMSO) were freshly prepared and diluted with cell culture medium to the desired concentrations (final DMSO concentration: 0.1% *v/v*, final complex concentrations: 100 and 500 μM). The cell culture medium of the cell culture flasks was replaced with 10 mL of the cell culture medium solutions containing the compounds, and the flasks were incubated at 37 °C under 5% CO_2 for 4 h. The culture medium was removed, the cell layer was washed with 10 mL phosphate buffered saline (PBS) at pH 7.4, treated with 2–3 mL trypsin solution (0.05% trypsin, 0.02% EDTA in PBS), and incubated for 2 min at 37 °C under 5% CO_2 after removal of the trypsin solution. Cells were resuspended in 10 mL PBS (in the case of **5**, the cells had to be scraped off using a flexible natural-rubber scraper attached to a glass rod—"rubber policeman") and isolated by centrifugation (room temperature, 2000 *g*, 5 min). The cell pellets were resuspended in 1.0 mL doubly distilled water, lysed by treatment with a sonotrode (Bandelin Sonoplus GM70, 60 W, 20 kHz, operated at 70% maximum power for 6–8 cycles), and appropriately diluted with doubly distilled water. The ruthenium content of the samples was determined by AAS (see below), and the protein content was determined by the Bradford method. Results were calculated as ng ruthenium per mg cellular protein from the data obtained in two independent experiments.

AAS measurements: A Vario 6 graphite furnace atomic absorption spectrometer (AnalytikJena AG) was used for ruthenium quantification. Ru was detected at a wavelength of 349.9 nm with a bandpass of 1.2 nm. A deuterium lamp was used for background correction. Standards for calibration purposes were prepared as aqueous dilutions of a commercially available ruthenium standard stock solution (Acros, 1 mg mL^{-1} ruthenium in 5% HCl). Triton X-100 (20 μL, 1%) and HCl (40 μL, 1 M) were added to each 160-μL sample or standard solution. A volume of 25 μL thereof was injected into the graphite tubes. Drying, pyrolysis, and atomization in the graphite furnace was performed according to the conditions listed in Table 2. The detection limit for the method was 4.8 μg Ru L^{-1}. The mean AUC (area under curve) absorptions of duplicate injections were used throughout the study.

Table 2. Graphite furnace program for ruthenium AAS measurements.

Step	*T* [°C]	Ramp [°C s^{-1}]	Hold [s]
drying	90	10	40
drying	105	7	30
drying	120	15	20
drying	500	50	30
pyrolysis	900	200	20
AZ (zeroing)	900	0	6
atomization	2200	maximum	4
tube cleaning	2600	1000	6

Cytotoxicity measurements: The antiproliferative effects of the compounds were determined following an established procedure. In short, cells were suspended in cell culture medium (HT-29: 2850 cells mL^{-1}, MCF-7: 10000 cells mL^{-1}), and 100-μL aliquots thereof were plated in 96-well plates and incubated at 37 °C under 5% CO_2 for 48 h (HT-29) or 72 h (MCF-7). Stock solutions of the compounds in DMSO were freshly prepared and diluted with cell culture medium to the desired concentrations (final DMSO concentration: 0.1% *v/v*). The medium in the plates was replaced with

medium containing the compounds in graded concentrations (six replicates). After further incubation for 72 h (HT-29) or 96 h (MCF-7) the cell biomass was determined by crystal violet staining, and the IC_{50} values were determined as concentrations that elicit 50% inhibition of cell proliferation. Results were calculated from two to three independent experiments.

Cell cultivation on the chip: HT-29 human colon carcinoma cells were kept in Dulbecco's modified Eagle's medium (DMEM) with penicillin/streptomycin and 10% (*v*/*v*) FCS. Cells were maintained at 37 °C under 5% CO_2 and 95% humidity. The same conditions were used to culture cells on the biosensor chips before insertion in the Bionas 2500 analyzer. During analysis, cells were fed with DMEM running medium (PAA, T15-178) without sodium bicarbonate, low buffered with 1 mM Hepes, supplemented with penicillin/streptomycin and 0.1% FCS. Approximately 1.5×10^5 cells were seeded directly onto each chip in 450 μL medium and incubated at 37 °C under 5% CO_2 and 95% humidity. The cell concentration used results in approximately 80% cell confluence on the chip surface after 24 h. This was the starting condition for online monitoring.

Bionas 2500 analyzing system and sensor chip: A Bionas 2500 analyzing system was used to continuously record three important physiological cellular parameters over time: oxygen consumption, change in medium pH, and the impedance between two electrodes on the chip surface. After short incubation periods the medium was exchanged. In this series of experiments, stop-and-go cycles of 4 min were used. The metabolic sensor chips (SC1000) include ion-sensitive field effect transistors (ISFETs) to record pH changes, oxygen electrodes to monitor oxygen consumption, and interdigitated electrode structures (IDES) to measure impedance under the cell layer.[33–35] For drug activity testing we included the three following steps: a) 4 h equilibration with running medium and 4-min stop/flow incubation intervals, b) drug incubation with substances freshly dissolved in medium at the indicated concentrations for treatment periods of up to 24 h, and c) a regeneration step in which cells are again fed with running medium only. At the end of each experiment, the cells were killed by addition of 0.2% Triton X-100 to get a basic signal without living cells on the sensor surface as a negative control.

Acknowledgements

This work was supported by the Deutsche Forschungsgemeinschaft (DFG) within FOR 630 "Biological function of organometallic compounds". U.S. thanks Prof. Dr. Nils Metzler-Nolte for generous access to all facilities of the institute.

Keywords: anticancer agents · bioinorganic chemistry · biological activity studies · ruthenium

[1] M. J. Clarke, *Coord. Chem. Rev.* **2003**, *236*, 209–233.
[2] I. Bratsos, S. Jedner, T. Gianferrara, E. Alessio, *Chimia* **2007**, *61*, 692–697.
[3] M. A. Jakupec, M. Galanski, V. B. Arion, C. G. Hartinger, B. K. Keppler, *Dalton Trans.* **2008**, 183–194.
[4] B. Lippert, *Cisplatin—Chemistry and Biochemistry of a Leading Anticancer Drug*, VCH, Weinheim, **1999**.
[5] E. Wong, C. M. Giandomenico, *Chem. Rev.* **1999**, *99*, 2451–2466.
[6] Y. Jung, S. J. Lippard, *Chem. Rev.* **2007**, *107*, 1387–1407.
[7] C. G. Hartinger, S. Zorbas-Seifried, M. A. Jakupec, B. Kynast, H. Zorbas, B. K. Keppler, *J. Inorg. Biochem.* **2006**, *100*, 891–904.
[8] E. Alessio, G. Mestroni, A. Bergamo, G. Sava, *Curr. Top. Med. Chem.* **2004**, *4*, 1525–1535.
[9] E. Corral, A. C. G. Hotze, A. Magistrato, J. Reedijk, *Inorg. Chem.* **2007**, *46*, 6715–6722.
[10] O. Novakova, J. Kasparkova, O. Vrana, P. M. van Vliet, J. Reedijk, V. Brabec, *Biochemistry* **1995**, *34*, 12369–12378.
[11] A. H. Velders, H. Kooijman, A. L. Spek, J. G. Haasnoot, D. de Vos, J. Reedijk, *Inorg. Chem.* **2000**, *39*, 2966–2967.
[12] K. Karidi, A. Garoufis, A. Tsipis, N. Hadjiliadis, H. den Dulk, J. Reedijk, *Dalton Trans.* **2005**, 1176–1187.
[13] Y. K. Yan, M. Melchart, A. Habtemariam, P. J. Sadler, *Chem. Commun.* **2005**, 4764–4776.
[14] M. Melchart, P. J. Sadler in *Bioorganometallics: Biomolecules, Labeling, Medicine* (Ed.: G. Jaouen), Wiley-VCH, Weinheim, **2006**, pp. 39–64.
[15] P. J. Dyson, *Chimia* **2007**, *61*, 698–703.
[16] S. J. Dougan, P. J. Sadler, *Chimia* **2007**, *61*, 704–715.
[17] S. Schäfer, I. Ott, R. Gust, W. S. Sheldrick, *Eur. J. Inorg. Chem.* **2007**, 3034–3046.
[18] K. E. Erkkila, D. T. Odom, J. K. Barton, *Chem. Rev.* **1999**, *99*, 2777–2795.
[19] C. Metcalfe, J. A. Thomas, *Chem. Soc. Rev.* **2003**, *32*, 215–224.
[20] B. M. Zeglis, V. C. Pierre, J. K. Barton, *Chem. Commun.* **2007**, 4565–4579.
[21] P. Lincoln, B. Norden, Int. Pat., WO 99/15535, **1999**.
[22] J. Liu, X.-H. Zou, Q.-L. Zhang, W.-J. Mei, J.-Z. Liu, L.-N. Ji, *Met.-Based Drugs* **2000**, *7*, 343–348.
[23] C. A. Puckett, J. K. Barton, *J. Am. Chem. Soc.* **2007**, *129*, 46–47.
[24] D.-L. Ma, C.-M. Che, F.-M. Siu, M. Yang, K.-Y. Wong, *Inorg. Chem.* **2007**, *46*, 740–749.
[25] G. I. Pascu, A. C. G. Hotze, C. Sanchez-Cano, B. M. Kariuki, M. J. Hannon, *Angew. Chem.* **2007**, *119*, 4452–4456; *Angew. Chem. Int. Ed.* **2007**, *46*, 4374–4378.
[26] B. H. Kim, D. N. Lee, H. J. Park, J. H. Min, Y. M. Jun, S. J. Park, W.-Y. Lee, *Talanta* **2004**, *62*, 595–602.
[27] S. Delaney, M. Pascaly, P. K. Bhattachary, K. Han, J. K. Barton, *Inorg. Chem.* **2002**, *41*, 1966–1974.
[28] A. Delgadillo, P. Romo, A. M. Leiva, B. Loeb, *Helv. Chim. Acta* **2003**, *86*, 2110–2120.
[29] X. W. Liu, J. Li, H. Deng, K. C. Zheng, Z. W. Mao, L. N. Ji, *Inorg. Chim. Acta* **2005**, *358*, 3311–3319.
[30] E. Amouyal, A. Homsi, J.-C. Chambron, J.-P. Sauvage, *J. Chem. Soc. Dalton Trans.* **1990**, 1841–1845.
[31] J. G. Collins, A. D. Sleeman, J. R. Aldrich-Wright, I. Greguric, T. W. Hambley, *Inorg. Chem.* **1998**, *37*, 3133–3141.
[32] Q.-L. Zhang, J.-H. Liu, J.-Z. Liu, P.-X. Zhang, X.-Z. Ren, Y. Liu, Y. Huang, L.-N. Ji, *J. Inorg. Biochem.* **2004**, *98*, 1405–1412.
[33] I. Ott, H. Scheffler, R. Gust, *ChemMedChem* **2007**, *2*, 702–707.
[34] R. Ehret, W. Baumann, M. Brischwein, A. Schwinde, K. Stegbauer, B. Wolf, *Biosens. Bioelectron.* **1997**, *12*, 29–41.
[35] R. Ehret, W. Baumann, M. Brischwein, M. Lehmann, T. Henningl, S. Freund, S. Drechsler, U. Friedrich, M. L. Hubert, E. Motrescu, A. Kob, H. Palzer, H. Grothe, B. Wolf, *Fresenius J. Anal. Chem.* **2001**, *369*, 30–35.
[36] E. Thedinga, A. Ullrich, S. Drechsler, R. Niendorf, A. Kob, D. Runge, A. Keuer, I. Freund, M. Lehmann, R. Ehert, *ALTEX* **2007**, *24*, 22–34.
[37] R. Gust, B. Schnurr, R. Krauser, G. Bernhardt, M. Koch, B. Schmid, E. Hummel, H. Schönenberger, *J. Cancer Res. Clin. Oncol.* **1998**, *124*, 585–597.
[38] H. E. Gottlieb, V. Kotlyar, A. Nudelman, *J. Org. Chem.* **1997**, *62*, 7512–7515.
[39] G. Mestroni, E. Alessio, G. Sava, Int. Pat., WO 98/00431, **1998**.

Received: February 14, 2008
Revised: March 18, 2008
Published online on April 18, 2008

